Astronomy and Space Science: Open Access
Received: Apr 17, 2018, Accepted: May11, 2018, Published: May 15, 2018
Astron Space Sci, Volume 4, Issue 1
http://crescopublications.org/pdf/ASSOA/ASSOA-4-013.pdf
Article Number: ASSOA-4-013

Research Article ISSN: 2472-9620 Open Access

Effect of Plasma Densities with Kappa Distribution Function on Electrostatic Ion Cyclotron Waves in Multi- Ions Plasma

Vibhooti Khaira* **and G. Ahirwar**

School of Studies in Physics, Vikram University, Ujjain (M.P.) 456010, India

***Corresponding author:** Vibhooti Khaira, School of Studies in Physics, Vikram University, Ujjain (M.P.) 456010, India, E-mail: khaira.vibhuti29@gmail.com

Citation: Vibhooti Khaira and G. Ahirwar (2018) Effect of Plasma Densities with Kappa Distribution Function on Electrostatic Ion Cyclotron Waves in Multi- Ions Plasma. Astron Space Sci 4: 013.

Abstract

Electrostatic ion-cyclotron (ESIC) waves have been studied by particle aspect approach. The effect of kappa distribution function with different plasma densities on ESIC instability in multi-ions is evaluated. The dispersion relation, growth rate of the electrostatic ion-cyclotron waves in a low β (ratio of plasma pressure to magnetic pressure), homogeneous plasma have been obtained. The influence of kappa distribution with different plasma densities on ESIC waves in multi-ions is to enhance the growth rate of ESIC waves. The outcomes are interpreted for the space plasma parameters appropriate to the auroral acceleration region of the earth's magneto-plasma

Keywords: Electrostatic ion-cyclotron wave; Particle aspect approach; Auroral acceleration region; Kappa distribution function; Multi-component plasma.bi-lorenzian distribution; Magnetosphere plasma.

1. Introduction

The ESIC waves can be produced by wave particle interactions in the magnetosphere and can be unglued into narrow band and broad band spectral types. Narrow band EIC waves typically reveal frequencies just above the proton cyclotron frequency and its harmonics. In a different way we can say an EIC wave is a longitudinal oscillation of ions and electrons in a magnetized plasma broadcasting closely (but not exactly) perpendicular to the magnetic field [2, 3].

The propagation of ESIC waves to the magnetosphere is powerfully affected by the ions (H^+) (He^+) and (O^+) [1]. The ESIC instability in the presence of cold plasma and contributed analytical expressions for the growth rates as a function of wave frequency. The numbers of authors worked at Beam-plasma interactions in the several space environments and in laboratory plasmas [4, 5]. The linear theory of plasma instabilities has been comprehensively studied in the past by several authors [4, 6-9].

We have also studied a systematic and detailed investigation of kappa distribution function on ESIC wave in multi-component (H^+) (He^+) and (O^+) with different plasma densities for magnetospheres like plasma parameters with the purpose of attaining a more complete understanding of their relative importance for this purpose we using the particle aspect approach in the presence of ESIC wave with kappa distribution function in multi-component magnetospheric plasma [10, 11].

For present analysis we are using particle aspect analysis which is the simplest approach for the single particle motion description it describes the motion of a particle under the influence of the external electric and magnetic fields. The detailed description and formulae for the dispersion relation and growth rate is determined in the next section.

2. Basic Assumption

The trajectories of particles are then evaluated within the framework of linear theory.

$$K_{\Pi}E, k = (k_{\perp}, 0, k_{\Pi}), \quad E = (E_x, 0, E_z)$$

With

$$E_x(r,t) = E_1 \cos(k_{\perp}x + k_{\Pi}z - \omega t),$$
$$E_z(r,t) = kE_1 \cos(k_{\perp}x + k_{\Pi}z - \omega t)$$

and

$$k = (\frac{k_{\Pi}}{k_{\perp}}) < 1$$

where

$$\phi = k_{\perp}x + k_{\Pi}z - \omega t$$

The amplitude E_1 is slowly varying function of t i.e $\frac{1}{E_1}(\frac{dE_1}{dt}) << \omega$

Here, $k_{\Pi}$and $k_{\perp}$are the components of the wave vector along and across the magnetic field, respectively and ω represent the wave frequency.

2.1 Velocities of the Particle

The trajectories of particles are evaluated within the framework of linear theory. The equation of motion of a particle is given by,

$$m\ (\frac{dv}{dt}) = q[E + (\frac{1}{c})v\ \times B_0] \qquad (1)$$

If E is considered to be a small perturbation i.e. $E=E_0+E_1$, velocity v can be expressed in terms of unperturbed velocity V and perturbed velocity u.

Then the trajectories of the free gyration are obtained as;

$$X(t) = \frac{V_{\perp}}{\Omega_{\alpha}}[\sin(\theta - \Omega_{\alpha}t) - \sin\theta] + Y_{0,}$$
$$Y(t) = \frac{V_{\perp}}{\Omega_{\alpha}}[\cos(\theta - \Omega_{\alpha}t) - \cos\theta] + Y_{0,} \qquad (2)$$
$$Z(t) = V_{\Pi}t + Z_{0,}$$

The perturbed velocity u is determined by;

$$\frac{du_{\perp}}{dt} + i\Omega_{\alpha}u_{\perp} = \frac{qk_{II}E_1}{k_{\perp}m}\sum_{-\infty}^{+\infty} J_1(\mu)\cos(A_{\lambda}t + \psi_{\lambda}{}^{0})$$
$$\frac{du_{\Pi}}{dt} = \frac{qE_1}{m}\sum_{-\infty}^{+\infty} J_1(\mu)\cos(A_{\lambda}t + \psi_{\lambda}{}^{0}) \quad (3)$$

Where $u_{\perp} = u_x + iu_y$ represents the perturbed velocity in transverse direction and $u_{\|}$represents the velocity in parallel direction. The resonance criteria are given by;

$$A_{\lambda}(V_{\Pi} = V_r) = k_{II}V_{II} - \omega + \lambda\Omega_{\alpha} = 0; \lambda = \pm 1, \pm 2, \pm 3, \ldots\ldots\ldots\ldots$$

Here, V_r is the resonance velocity of the particles.

The oscillatory solution of u (t) is given by;

$$u_x(\rho.t) = -\frac{qE_1}{m}\sum_{-\infty}^{+\infty} J_n(\mu)\times\left[\frac{A_{\lambda}}{A_{\lambda} - \Omega^2{}_{\alpha}}\sin\chi_{nl} - \frac{\delta}{2A_{n+1}}\sin(\chi_{nl} - A_{n+1}t) - \frac{\delta}{2A_{n-1}}\sin(\chi_{nl} - A_{n-1}t)\right]$$

$$u_y(\rho.t) = \frac{qE_1}{m}\sum_{-\infty}^{+\infty} J_n(\mu)\sum_{-\infty}^{+\infty} J_{\lambda}(\mu)\times\left[\frac{A_{\lambda}}{A^2{}_{\lambda} - \Omega^2{}_{\alpha}}\cos\chi_{nl} - \frac{\delta}{2A_{n+1}}\cos(\chi_{nl} - A_{\lambda+1}t) - \frac{\delta}{2A_{\lambda-1}}\sin(\chi_{nl} - A_{\lambda-1}t)\right] \quad (4)$$

$$u_z(\rho.t) = \frac{qk_{II}E_1}{k_{\perp}m}\sum_{-\infty}^{+\infty} J_n(\mu)\sum_{-\infty}^{+\infty} J_{\lambda}(\mu)\times\frac{1}{A_{\lambda}}\left[\sin\chi_{nl} - \delta\sin(\chi_{nl} - A_{n+1}t)\right]$$

Here

$$\chi_{nl} = k.r - \omega t + (n - \lambda)(\Omega_{\alpha}t - \theta)$$

δ =0 for non-resonant particles and δ =1for resonant particles.

2.2 Distribution Function:

To determine the dispersion relation and growth rate, we consider bi-Maxwellian plasma as,

$$f_0(y, V) = N_0 f_{\perp}(V_{\perp}) f_{\Pi}(V_{\Pi}) \quad (5)$$

We consider a general loss-cone distribution function for $f_{\perp}(V_{\perp})$ as

$$f_{\perp}(V_{\perp}) = \left[\frac{V^{2J}{}_{\perp}}{\pi V_{T\perp}{}^{2(J+1)}}\right]\exp\left(-\frac{V^2{}_{\perp}}{V_{T\perp}{}^2}\right) \quad (6)$$

And $f_{\|}(V_{\|})$which is defined by the drifting Maxwellian as

$$f_{II}(V_{II}) = \left[\frac{V^{2J}{}_{II}}{\sqrt{\pi}V_{II\perp}{}^{2(J+1)}}\right]\exp\left(-\frac{V^2{}_{II}}{V_{TII}{}^2}\right) \quad (7)$$

Here using the value of $V^2{}_{T\perp} = (J+1)^{-1}\frac{2T_{\perp}}{m}$ and $V^2{}_{TII} = \frac{2T_{II}}{m}$ for plasma and the bi-lorentzian, which reduces to the anisotropic bi-maxwellian distribution when the spectral index k tends to infinity is given by,

$$F = \frac{1}{\sqrt[3]{\pi}}\frac{\Gamma(\kappa + J + 1)}{\sqrt[3]{\kappa}\Gamma\kappa - 1/2V^2{}_{T\perp}V^2{}_{TII}}[1 + \frac{V^2{}_{T\perp}}{KV^2{}_{T\perp}} + \frac{V^2{}_{TII}}{KV^2{}_{TII}}]^{-(\kappa+J+1)} \quad (8)$$

In equation (8) $V^2{}_{T\perp}$ and $V^2{}_{TII}$ are related to the mass m and the temperatures $T_\perp$ and T_{II} respectively parallel and perpendicular to the magnetic field by,

$$V^2{}_{T\perp} = (J+1)^{-1}[\frac{\kappa - 3/2}{\kappa}\frac{2KT_\perp}{m}] \quad (9)$$

$$V^2{}_{TII} = [\frac{\kappa - 3/2}{\kappa}\frac{2KT_{II}}{m}] \quad (10)$$

The quasi-neutrality condition yields to the equation:

$$n_e = n_{H^+} + n_{He^+} + n_{O^+}$$

Thus we evaluate the density perturbation associated with the particle velocity as:

$$\frac{dn_1}{dt} = -F_{H^+}(V)(\nabla.u)_{H^+} + (-F_{He^+}(V)(\nabla.u)_{He^+} + (-F_{O^+}(V)(\nabla.u)_{O^+} \quad (11)$$

The integration w.r.to t from equation (8) we get the solution for perturbed density as

$$n_1(r,t) = -\frac{qE_1F(V_\alpha)}{m_\alpha k^2{}_\perp}k_{II}{}^2\sum_{-\infty}^{+\infty}J_\lambda(\mu)J_n(\mu)\times[\frac{k_\perp}{\mathrm{A}^2{}_\lambda - \Omega^2{}_\alpha} + \frac{k_{II}{}^2K_\perp}{k^2{}_\perp A^2{}_\lambda}]\sin\chi_{nl}$$

And

$$n_1(r,t) = \frac{qE_1F(V_{H^+})}{m_{H^+}k_\perp{}^2}k_{II}{}^2K_\perp\sum_{\lambda,n=-\infty}^{+\infty}J_\lambda(\mu)J_n(\mu)\frac{1}{\mathrm{A}^2{}_{\lambda H^+}}\left\{\sin(\chi_{n\lambda} - \sin(\chi_{n\lambda} - A_{\lambda H^+}t) - A_{\lambda H^+}t\cos(\chi_{n\lambda} - A_{\lambda H^+}t)\right\} +$$
$$\frac{qE_1F(V_{He^+\alpha})}{m_{He^+}k_\perp{}^2}k_{II}{}^2K_\perp\sum_{\lambda,n=-\infty}^{+\infty}J_\lambda(\mu)J_n(\mu)\frac{1}{\mathrm{A}^2{}_{\lambda He^+}}\left\{\sin(\chi_{n\lambda} - \sin(\chi_{n\lambda} - A_{\lambda He^+}t) - A_{\lambda He^+}t\cos(\chi_{n\lambda} - A_{\lambda He^+}t)\right\} +$$
$$\frac{qE_1F(V_{O^+})}{m_{O^+}k^2{}_\perp}k_{II}{}^2K_\perp\sum_{\lambda,n=-\infty}^{+\infty}J_\lambda(\mu)J_n(\mu)\frac{1}{\mathrm{A}^2{}_{\lambda O^+}}\left\{\sin(\chi_{n\lambda} - \sin(\chi_{n\lambda} - A_{\lambda O^+}t) - A_{\lambda O^+}t\cos(\chi_{n\lambda} - A_{\lambda O^+}t)\right\} \quad (12)$$

3. Dispersion Relation

We consider the cold plasma dispersion relation for the ESIC wave as;

$$n_{\alpha,e} = \mu\int dvF(v)\frac{eE_1K_\perp}{m_{\alpha,e}}\sum_{n\lambda}\left\{J_\lambda(\mu)J_n(\mu)\times[\frac{K_\perp}{\mathrm{A}^2{}_\lambda - \Omega^2{}_\alpha} + \frac{k_{II}{}^2}{k^2{}_\perp A^2{}_\lambda}]\sin\chi_{nl}\right\} \quad (13)$$

Where $n_{\alpha,e}$ is integrated density and

$$\mu = \frac{K_\perp V_\perp}{\Omega_{\alpha,e}}, \mathrm{A} = K_{II}V_{II} - \omega + n\Omega_{i,e}, \chi_{n\lambda} = k.r - \omega t + (n-l)(\Omega_\alpha l - \theta)$$

Using the expression, then the dispersion relation EIC waves in multi-component plasma is given by

$$n_e = (\frac{1}{k_\perp d^2{}_{IIe}})\frac{E_1}{4\pi e}\sin(kr - \omega t)$$

$$n_\alpha = -\frac{{k_{II}}^2 \omega^2{}_{p\alpha} 1}{(\omega - \lambda\Omega_\alpha)k_\perp}\left\langle 1 - \frac{k^2{}_\perp \rho^2{}_\alpha}{2}\left(\frac{2\kappa - 3}{\kappa}\right)\right\rangle \frac{E_1}{4\pi e}\sin(kr - \omega t)$$

And

Where $\alpha = \mathrm{H}^+, \mathrm{He}^+, \mathrm{O}^+ and \omega^2{}_{p\alpha} = \frac{4\pi N_\alpha e^2}{m_\alpha}$ is the plasma frequency for multi-ions and N_α is the multi-ions plasma density.

Debye length ($d^2{}_{IIe}$) is given by

$$d^2{}_{IIe} = \frac{T_{IIe}}{m_e \omega^2{}_{pe}}$$

Using the Poisson's equation

$$\nabla . E = 4\pi e(n_\alpha - n_{e)} \quad (14)$$

The perturbed ion and electron density ni and ne the dispersion relation is obtain as

$$\omega = \Omega_\alpha + [\frac{4\pi N_\alpha e^2}{m_\alpha}\left\langle 1 - \frac{k^2{}_\perp \rho^2{}_\alpha}{2}\left(\frac{2\kappa - 3}{\kappa}\right)\right\rangle (\frac{1}{\frac{k_\perp + k_{II}}{{k_{II}}^2 k_\perp} + \frac{k^2{}_\perp}{{k_{II}}^2}(\frac{1}{k^2{}_\perp d^2{}_{IIe}})}) \quad (15)$$

4. Wave Energy and Growth Rate

The wave energy W_w per unit wavelength is the sum of the pure field energy. The total energy per unit wavelength is given as

$$W_w = \frac{\lambda B^2}{8\pi} + W_e + W_{r\alpha}$$

Where $W_e = \frac{\lambda E^2}{8\pi} + \frac{\lambda E^2}{16\pi}(\frac{1}{k_\perp d^2{}_{IIe}})$

$$W_{r\alpha} = \sum_\alpha (W_{r\alpha\perp} + W_{r\alpha II})$$

and $$W_{r\perp} = \int_0^\lambda dz \int_0^\infty V_{\perp\alpha} dV_{\perp\alpha} \int_0^{2\theta} d\theta \int_{v_r - \Delta r}^{v_r + \Delta r} dV_{\Pi\alpha} \frac{m}{2}[(N + n_{1\alpha})(V_{\perp\alpha} + u_{\perp\alpha})^2 - N{V_{\perp\alpha}}^2] \quad (16)$$

$$W_{rII} = \int_0^\lambda dz \int_0^\infty V_{II\alpha} dV_{II\alpha} \int_0^{2\theta} d\theta \int_{v_r - \Delta r}^{v_r + \Delta r} dV_{\Pi\alpha} \frac{m}{2}[(N + n_{1\alpha})(V_{II\alpha} + u_{II\alpha})^2 - N{V_{II\alpha}}^2]$$

4.1 Perpendicular Resonant Energy

$$W_{r\perp\alpha} = (\frac{\lambda E^2}{8\pi})(\frac{4\pi N_\alpha e^2}{{\Omega_\alpha}^2 m_\alpha})(\frac{\omega}{k_{II} V_{th\alpha}})\frac{\Omega_\alpha t}{\sqrt{2\pi}}\exp\left\{-\frac{1}{2}(\frac{\omega}{k_{II} V_{th\alpha}})^2(1 - \frac{\lambda\Omega_\alpha}{\omega})^2\right\} \times \frac{1}{2}\left\langle 1 - \frac{k^2{}_\perp \rho^2{}_\alpha}{2}\left(\frac{2\kappa - 3}{\kappa}\right)\right\rangle$$

$$\left[1 - (\frac{R(\frac{\lambda\Omega_\alpha}{\omega} - 1)}{\frac{\lambda\Omega_\alpha}{\omega}})\frac{T_{\perp\alpha}}{T_{II\alpha}}\right]$$

(17)

4.2 Parallel Resonant Energy

$$W_{r\parallel\alpha} = \left(\frac{\lambda E^2}{8\pi}\right)\left(\frac{4\pi N_\alpha e^2}{\Omega_\alpha{}^2 m_\alpha}\right)\left(\frac{\omega}{k_\parallel V_{th\alpha}}\right)\frac{\Omega_\alpha t}{\sqrt{2\pi}}\exp\left\{-\frac{1}{2}\left(\frac{\omega}{k_\parallel V_{th\alpha}}\right)^2\left(1-\frac{\lambda\Omega_\alpha}{\omega}\right)^2\right\}\times\frac{1}{2}\left\langle 1-\frac{k^2{}_\perp\rho^2{}_\alpha}{2}\left(\frac{2\kappa-3}{\kappa}\right)\right\rangle$$
$$\left[\frac{\left(\frac{\lambda\Omega_\alpha}{\omega}-1\right)}{\left(\frac{\omega}{\lambda\Omega_\alpha}\right)}\frac{T_{\perp\alpha}}{T_{\parallel\alpha}}\right] \qquad (18)$$

Where

$$R=\frac{1-\frac{1}{2}\frac{k^2{}_\perp\rho^2{}_\alpha}{2}\left(\frac{2\kappa-3}{\kappa}\right)}{1-\frac{k^2{}_\perp\rho^2{}_\alpha}{2}\left(\frac{2\kappa-3}{\kappa}\right)} \text{ and } \alpha = H^+, He^+, O^+$$

4.3 Growth Rate

Using the law of conservation of energy the growth rate is obtained as

$$\frac{\gamma}{\omega}=\sqrt{\frac{\pi}{2}}\left(\frac{\omega}{k_\parallel V_{th\alpha}}\right)\left(1-\frac{\lambda\Omega_\alpha}{\omega}\right)^2\exp\left\{-\frac{1}{2}\left(\frac{\omega}{k_\parallel V_{th\alpha}}\right)^2\left(1-\frac{\lambda\Omega_\alpha}{\omega}\right)^2\right\}\times\left[R\left(\frac{\frac{\lambda\Omega_\alpha}{\omega}-1}{\frac{\lambda\Omega_\alpha}{\omega}}\right)\frac{T_{\perp\alpha}}{T_{\parallel\alpha}}-1\right] \qquad (19)$$

5. Results and Discussion

The role of ESIC in multicomponent plasma wave particle interaction in the auroral acceleration region is examined in the present analysis. The characteristics of the ESIC waves were derived by using auroral acceleration region.

$B_o = 4300nT\ at\ 1.4R_E, K_\perp \approx 2.5\times10^{-3}m^{-1},, \omega_{pH}^2 = 1.552\times10^9 sec^{-2},$

$\omega_{pHe}^2 = .216\times10^8 sec^{-2}, \omega_{pO}^2 = .05\times10^8 sec^{-2}$

$\Omega_H = 412 sec^{-2}, \Omega_{He} = 103 sec^{-2}, \Omega_O = 26 sec^{-2}, \frac{T_\perp}{T_\parallel} = 50, k_B T_\parallel = 5eV.$

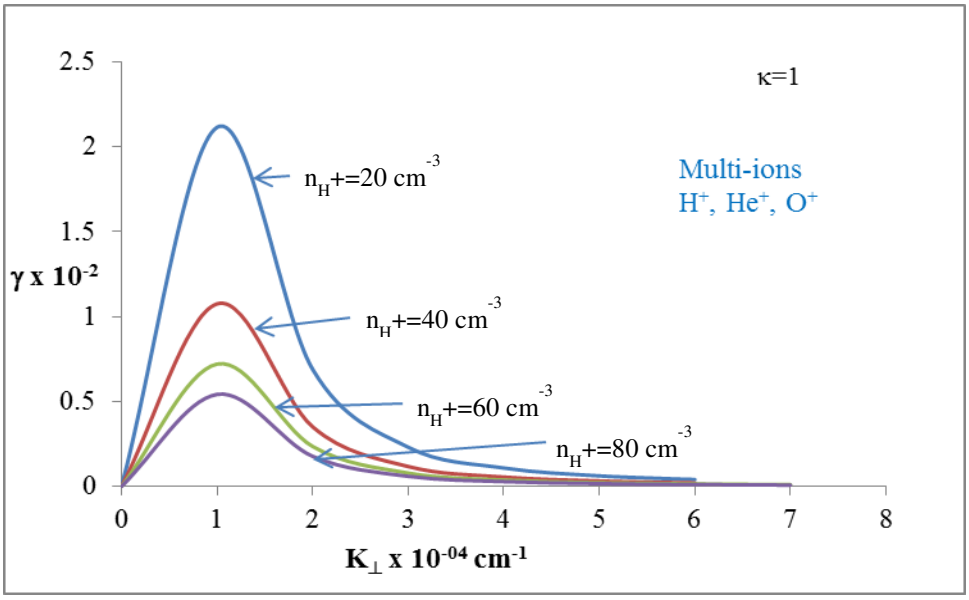

Figure 1: Shows the variation of growth rate versus wave vector (cm^{-1}) for different values of plasma densities of hydrogen ions ($n_{H^+} = 20, 40, 60, 80$) cm^{-3} for kappa distribution function k=1.

Figure 1 shows the variation of growth rate versus wave vector (cm^{-1}) for different values of plasma densities of hydrogen ions ($n_{H^+} = 20, 40, 60, 80$) cm^{-3} for kappa distribution function k=1. It is observed that growth rate is increases at particular value of wave vector for decreasing values of plasma densities of hydrogen ions. As we increase the value of wave vector growth rate decreasing with decreasing hydrogen density for kappa distribution function k=1.

In Figure 2, it is observed that growth rate is decreasing for decreasing of plasma densities of hydrogen ions for higher value of kappa distribution k=2. It means effect of kappa function is to enhance the growth rate for different values of plasma densities of hydrogen ions. This implies that for minimum value of hydrogen densities we get minimum growth rate.

Figure 3 shows the variation of growth rate versus wave vector (cm^{-1}) for different values of plasma densities of helium ions ($n_{He^+} = 20, 40, 60, 80$) cm^{-3} for kappa distribution function k=1. It is observed that for kappa distribution k=1, growth rate increases at particular value of wave vector for different values of plasma densities of helium ions respectively. After that decrease the value of growth rate with increasing the value of wave vector. Which means that decreasing the value of plasma densities of helium ions growth rate increases with respect to wave vector for k=1. At particular value of wave vector growth rate is zero for all plasma densities of hydrogen ions.

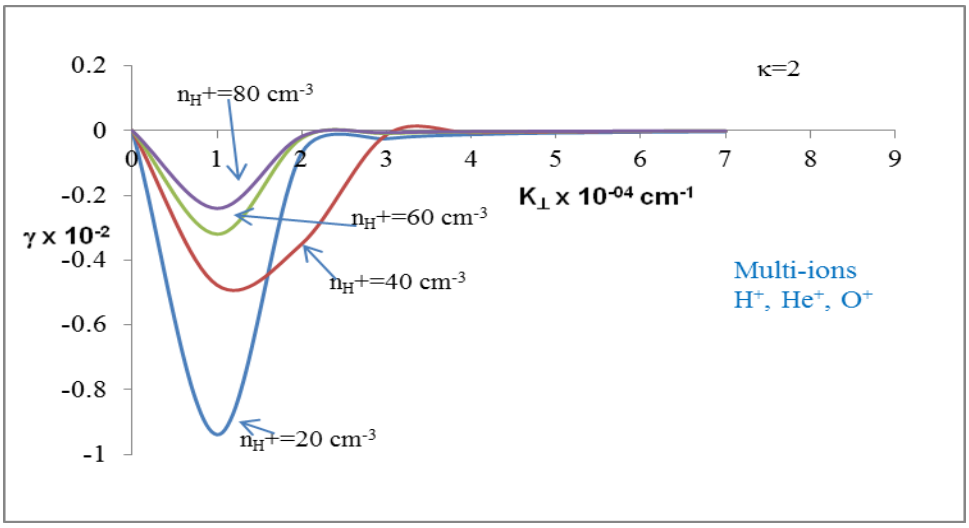

Figure 2: Shows the variation of growth rate versus wave vector (cm^{-1}) for different values of plasma densities of hydrogen ions ($n_{H^+} = 20, 40, 60, 80$) cm^{-3} for kappa distribution function k=2.

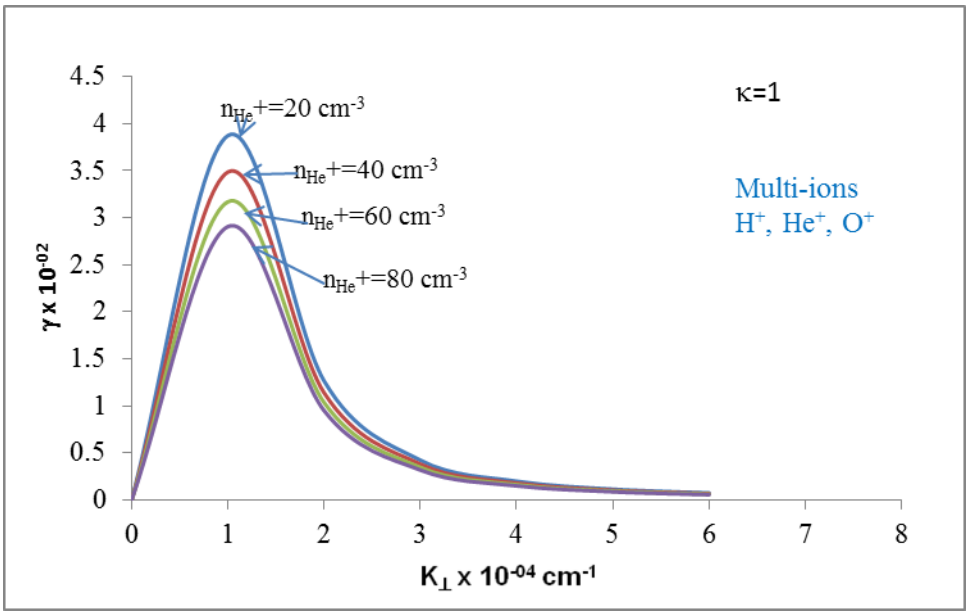

Figure 3: Shows the variation of growth rate versus wave vector (cm^{-1}) for different values of plasma densities of helium ions ($n_{He^+} = 20, 40, 60, 80$) cm^{-3} for kappa distribution function k=1.

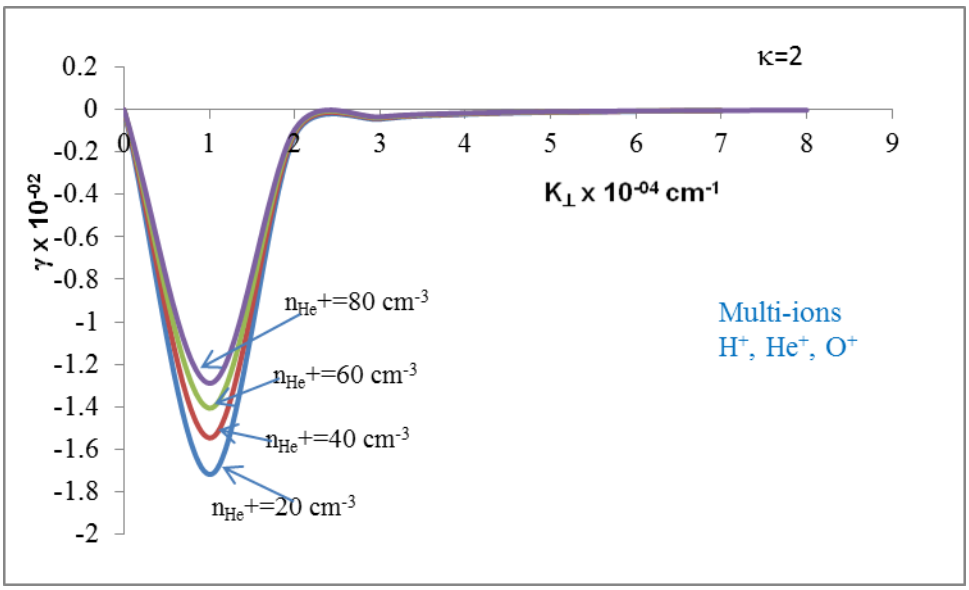

Figure 4: Shows the variation of growth rate versus wave vector (cm^{-1}) for different values of plasma densities of helium ions ($n_{He^+} = 20, 40, 60, 80$) cm^{-3} for kappa distribution function k=2.

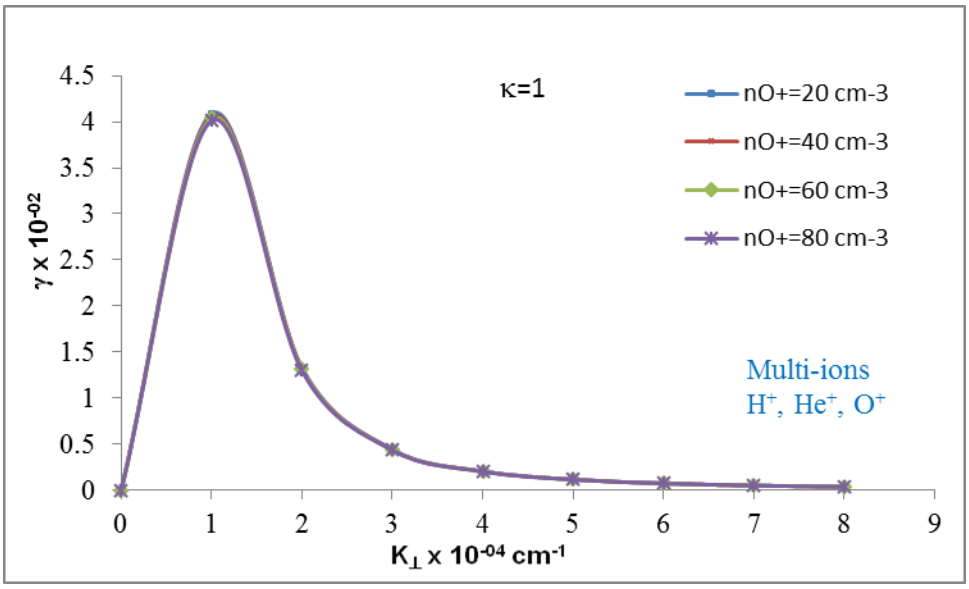

Figure 5: Shows the variation of growth rate versus wave vector (cm^{-1}) for different values of plasma densities of oxygen ions ($n_{O^+} = 20, 40, 60, 80$) cm^{-3} for kappa distribution function k=1.

Figure 4 shows the variation of growth rate versus wave vector (cm^{-1}) for different values of plasma densities of helium ions ($n_{He^+} = 20, 40, 60, 80$) cm^{-3} for kappa distribution function k=2. It is observed that for k=2 increasing the value of plasma densities of helium ions, growth rate increases with respect to wave vector.

Figure 5 shows the variation of growth rate versus wave vector (cm^{-1}) for different values of plasma densities of oxygen ions ($n_{O^+} = 20, 40, 60, 80$) cm^{-3} for kappa distribution function k=1. It is observed that for the value of growth rate is increasing with particular wave vector for different values of plasma densities of oxygen ions. Here we have seen that for different values of plasma densities growth is same with respect to wave vector.

Figure 6 shows the variation of growth rate versus wave vector (cm^{-1}) for different values of plasma densities of oxygen ions ($n_{O^+} = 20, 40, 60, 80$) cm^{-3} for kappa distribution function k=2. Here it is observed that for k=2 growth rate is same for all values of plasma densities of oxygen. Also we have seen that growth rate is to enhance the increasing value of wave vector.

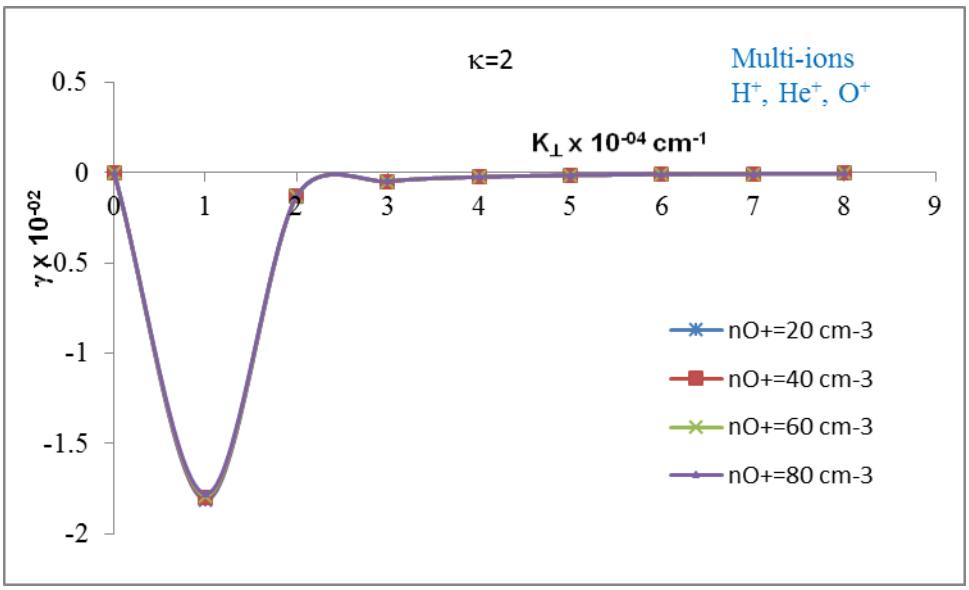

Figure 6: Shows the variation of growth rate versus wave vector (cm^{-1}) for different values of plasma densities of oxygen ions ($n_{O^+} = 20, 40, 60, 80$) cm^{-3} for kappa distribution function k=2.

Here in Figures 1-6 we observed that for k=1 growth is enhancing according to wave vector as decreasing the plasma density of different ions. For k=2 we get minimum growth rate as we increase the plasma densities of different ions. For hydrogen and helium ions we get different growth rate according to wave vector at different densities of oxygen ions for k=1 and 2. But for oxygen ions we get same growth rate according to wave vector at different densities of oxygen ions. Energy can be transferred between the particles and waves when the particles gyro-frequency matches the Doppler shifted wave frequency. The effective amplification of ESIC waves depends on the amount of time spent propagating through a finite growth region. Thus the kappa distribution enhances the wave emission of ESIC mode as well as controls the heating of the ions parallel and perpendicular to the magnetic field. The mirroring force may be operative in association with ESIC wave to control the heating and to emit the wave.

Figure 7 shows the variation of perpendicular resonant energy (erg cm) versus wave vector (cm^{-1}) for different values of plasma densities of hydrogen ions ($n_{H^+} = 20, 40, 60, 80$) cm^{-3} for kappa distribution function k=1. It is seen that for different plasma densities of hydrogen ions, perpendicular resonant energy increases with respect to wave vector. As we increase the value of plasma densities of hydrogen growth rate enhance with wave vector.

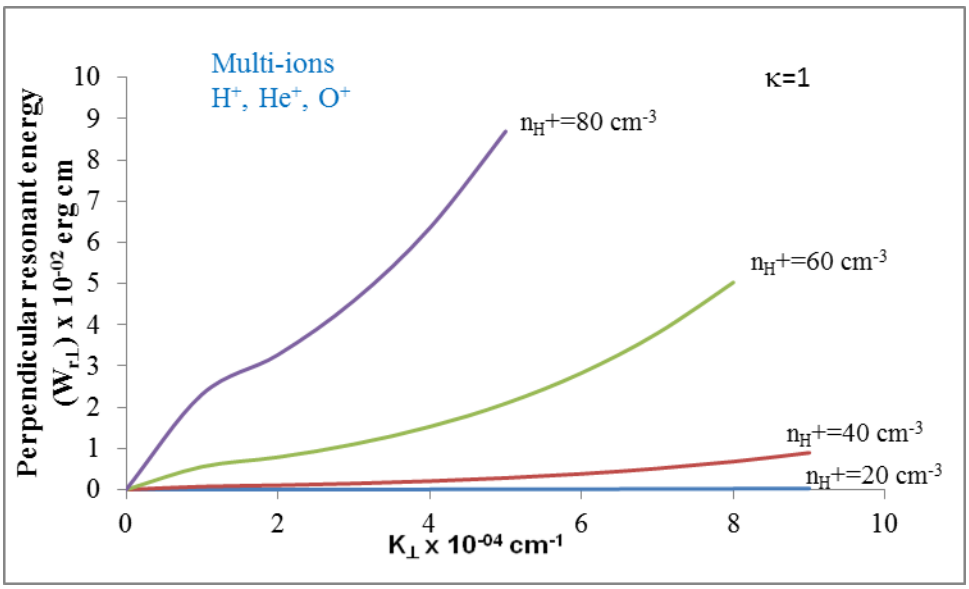

Figure 7: Shows the variation of perpendicular resonant energy (erg cm) versus wave vector (cm^{-1}) for different values of plasma densities of hydrogen ions ($n_{H^+} = 20, 40, 60, 80$) cm^{-3} for kappa distribution function k=1.

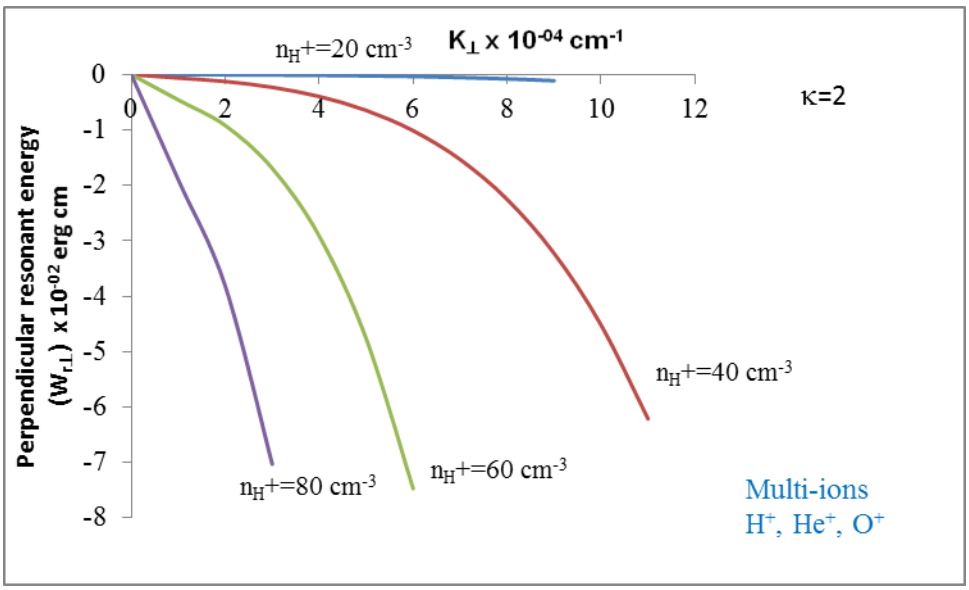

Figure 8: Shows the variation of perpendicular resonant energy (erg cm) versus wave vector (cm^{-1}) for different values of plasma densities of hydrogen ions ($n_{H^+} = 20, 40, 60, 80$) cm^{-3} for kappa distribution function k=2.

Figure 8 shows the variation of perpendicular resonant energy (erg cm) versus wave vector (cm^{-1}) for different values of plasma densities of hydrogen ions ($n_{H^+} = 20, 40, 60, 80$) cm^{-3} for kappa distribution function k=2. It is observed that perpendicular resonant energy decreases with increase of wave vector.

Figure 9 shows the variation of perpendicular resonant energy (erg cm) versus wave vector (cm^{-1}) for different values of plasma densities of helium ions ($n_{He^+} = 20, 40, 60, 80$) cm^{-3} for kappa distribution function k=1. It is observed that lower value of plasma density we get minimum resonant energy as we increase the value of plasma density we get maximum value of perpendicular resonant energy with respect to wave vector. Which implies that perpendicular resonant energy is increasing with increase of plasma densities of hydrogen for minimum value of kappa k=1.

Figure 10 shows the variation of perpendicular resonant energy (erg cm) versus wave vector (cm^{-1}) for different values of plasma densities of helium ions ($n_{He^+} = 20, 40, 60, 80$) cm^{-3} for kappa distribution function k=2. For maximum value of k we get minimum value of perpendicular resonant energy for higher value of plasma densities of helium corresponding with wave vector. Which implies that growth rate is decreasing with increasing the value of plasma densities of helium ions with respect to wave vector.

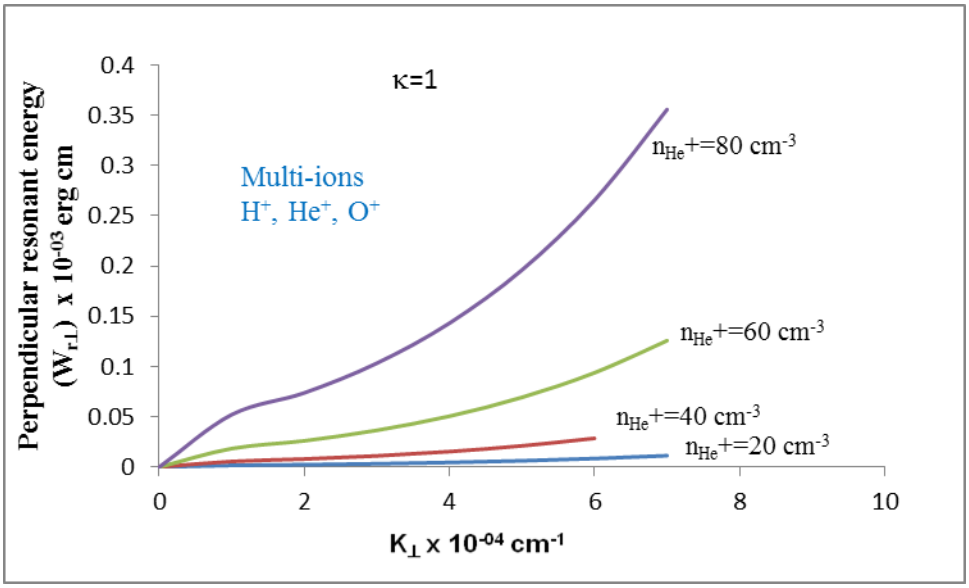

Figure 9: Shows the variation of perpendicular resonant energy (erg cm) versus wave vector (cm^{-1}) for different values of plasma densities of helium ions ($n_{He^+} = 20, 40, 60, 80$) cm^{-3} for kappa distribution function k=1.

Here in Figures 7-12 we observed that for k=1 we get maximum perpendicular resonant energy according to wave vector for different plasma densities of ions and we have seen for maximum value of ion densities we get maximum resonant energy. It can be concluded that perpendicular resonant energy increases with increasing the plasma densities of ions. The kappa distribution function enhances the perpendicular resonant energy with multi-ions plasma which supports the wave emissions and controls the heating of ions to parallel and perpendicular resonant energy to the magnetic field. Mirroring force may also be useful in the generation of EIC waves and controlling the heating of ions. The kappa distribution can acts as a source of free energy for the generation of ESIC waves in multi-ions plasma

For k=2 we get minimum perpendicular resonant energy according to wave vector for multi-ions densities which implies that perpendicular heating of resonant ions decreases at a particular wave number at which energy is decreased. Perpendicular heating earlier studied by Hamrin [12] and Albert [13]. Transverse acceleration of ions may be due to damping of the ESIC waves not by the amplification.

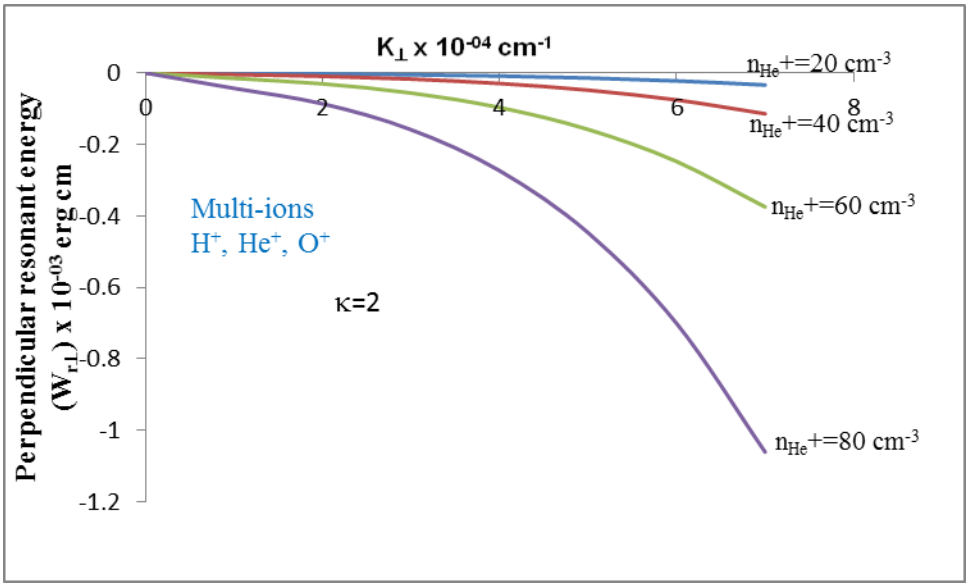

Figure 10: Sows the variation of perpendicular resonant energy (erg cm) versus wave vector (cm^{-1}) for different values of plasma densities of helium ions ($n_{He^+} = 20, 40, 60, 80$) cm^{-3} for kappa distribution function k=2.

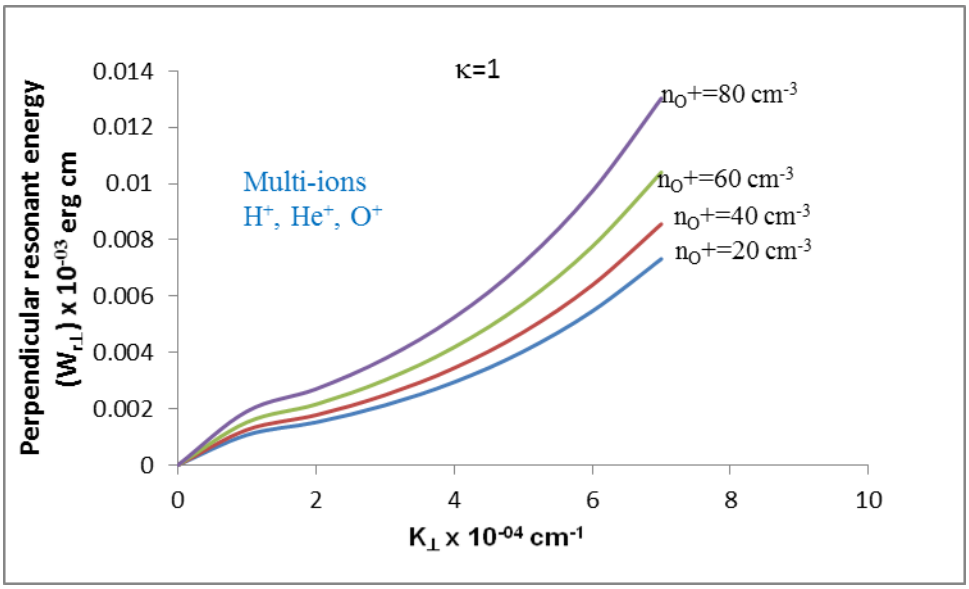

Figure 11: Shows the variation of perpendicular resonant energy (erg cm) versus wave vector (cm^{-1}) for different values of plasma densities of oxygen ions ($n_{O^+} = 20, 40, 60, 80$) cm^{-3} for kappa distribution function k=1.

Figures 11 and 12 show the variation of perpendicular resonant energy (erg cm) versus wave vector (cm^{-1}) for different values of plasma densities of oxygen ions ($n_{O^+} = 20, 40, 60, 80$) cm^{-3} for different kappa distribution function k=1 and 2. For k=1 perpendicular resonant energy exponentially increases with increasing value of plasma density of oxygen ions with respect to wave vector. For k=2 perpendicular resonant energy decreases with increasing value of plasma densities of oxygen ions corresponding to the wave vector. It means for maximum value of plasma density of oxygen ions we get minimum value of resonant energy for k=2.

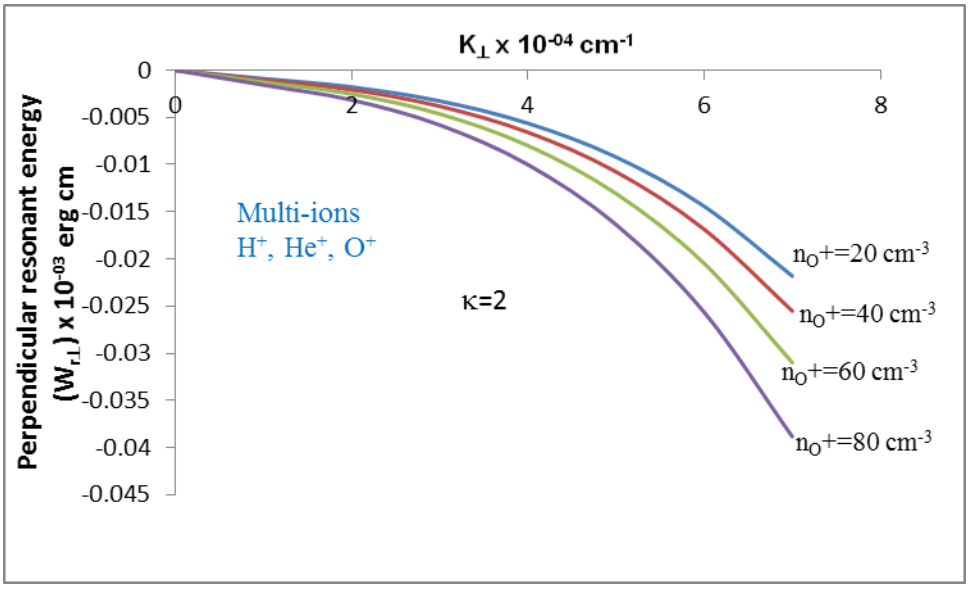

Figure 12: Shows the variation of perpendicular resonant energy (erg cm) versus wave vector (cm^{-1}) for different values of plasma densities of oxygen ions ($n_{O^+} = 20, 40, 60, 80$) cm^{-3} for kappa distribution function k=2.

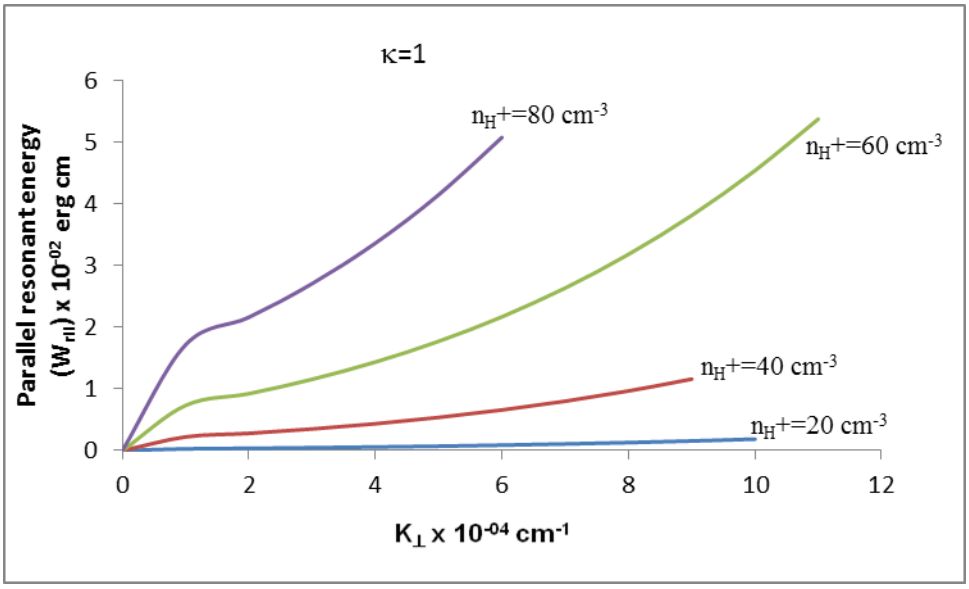

Figure 13: Shows the variation of parallel resonant energy (erg cm) versus wave vector (cm^{-1}) for different values of plasma densities of hydrogen ions ($n_{H^+} = 20, 40, 60, 80$) cm^{-3} for kappa distribution function k=1.

Figures 13 and 14 show the variation of parallel resonant energy (erg cm) versus wave vector (cm^{-1}) for different values of plasma densities of hydrogen ions ($n_{H^+} = 20, 40, 60, 80$) cm^{-3} for kappa distribution function k=1 and 2. Here we observed that parallel resonant energy increases with increases of plasma densities of hydrogen ions with respect to wave vector for all kappa distribution k=1 and 2. This implies that different values of plasma densities of hydrogen ions raise the parallel resonant energy.

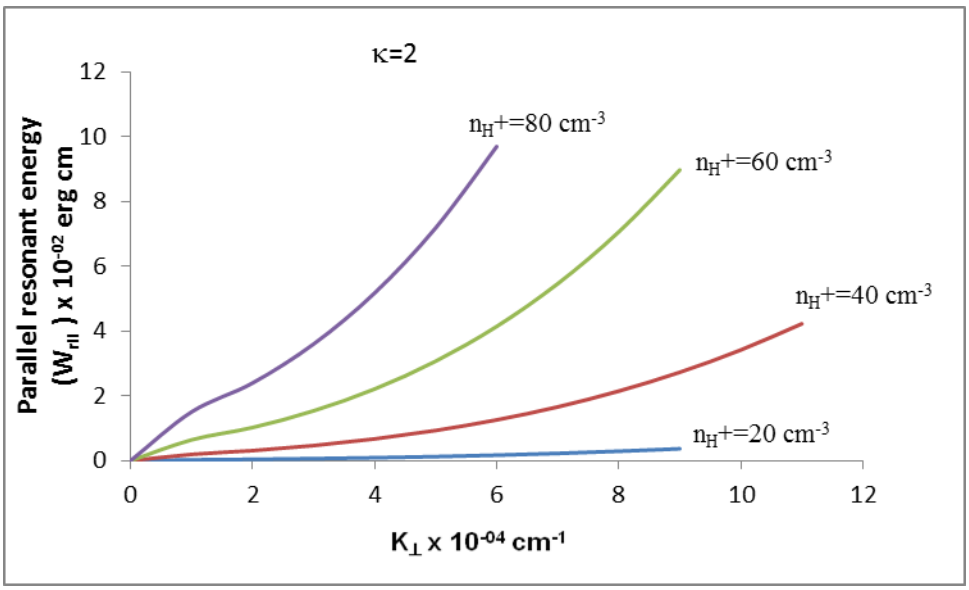

Figure 14: Shows the variation of parallel resonant energy (erg cm) versus wave vector (cm^{-1}) for different values of plasma densities of hydrogen ions ($n_{H^+} = 20, 40, 60, 80$) cm^{-3} for kappa distribution function k=2.

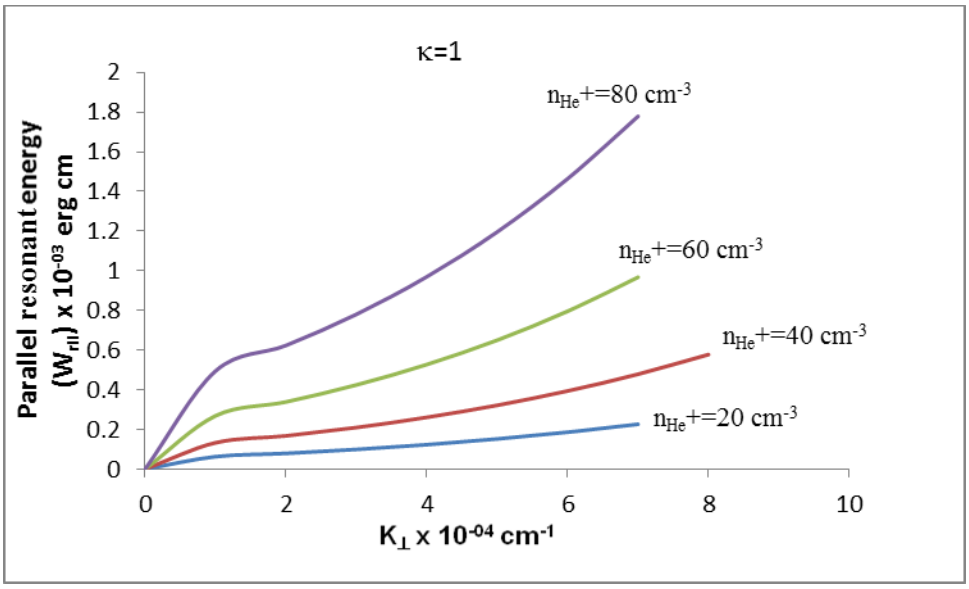

Figure 15: Shows the variation of parallel resonant energy (erg cm) versus wave vector (cm^{-1}) for different values of plasma densities of helium ions ($n_{He^+} = 20, 40, 60, 80$) cm^{-3} for kappa distribution function k=1.

Figures 15 and 16 show the variation of parallel resonant energy (erg cm) versus wave vector (cm^{-1}) for different values of plasma densities of helium ions ($n_{He^+} = 20, 40, 60, 80$) cm^{-3} for kappa distribution function k=1 and 2. We have seen that for value of k=1 and 2 parallel resonant energy is approximately equal increases with increase of plasma densities of helium ions with respect to wave vector.

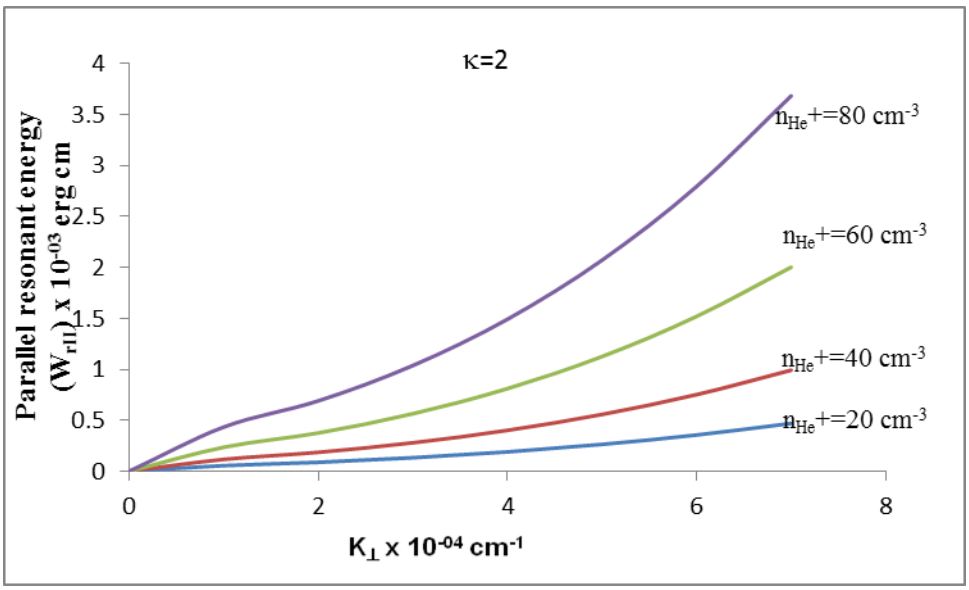

Figure 16: Shows the variation of parallel resonant energy (erg cm) versus wave vector (cm^{-1}) for different values of plasma densities of helium ions ($n_{He^+} = 20, 40, 60, 80$) cm^{-3} for kappa distribution function k=2.

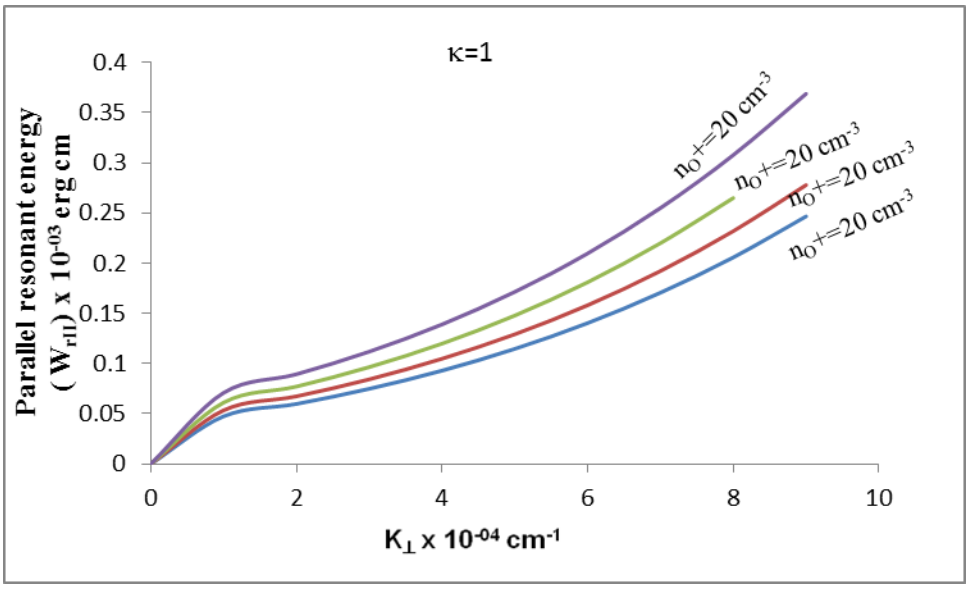

Figure 17: Shows the variation of parallel resonant energy (erg cm) versus wave vector (cm^{-1}) for different values of plasma densities of oxygen ions ($n_{O^+} = 20, 40, 60, 80$) cm^{-3} for kappa distribution function k=1.

Figures 17 and 18 show the variation of parallel resonant energy (erg cm) versus wave vector (cm^{-1}) for different values of plasma densities of oxygen ions ($n_{O^+} = 20, 40, 60, 80$) cm^{-3} for kappa distribution function k=1 and 2.here we observed that both values of parallel resonant energy is same with respect to wave vector for different value of k=1 and 2.

Here we have seen for k=1 and 2 parallel resonant energy increases with increase of plasma densities of different ions (H^+, He^+, O^+) according to wave vector. This may be due to mirroring effect of ions and interchange of energy between particle and wave.

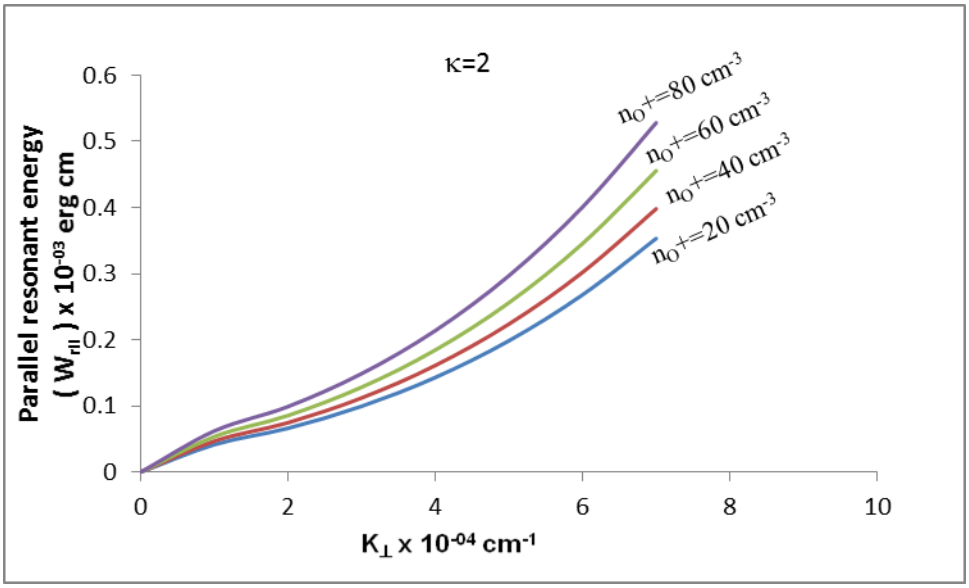

Figure 18: Shows the variation of parallel resonant energy (erg cm) versus wave vector (cm^{-1}) for different values of plasma densities of oxygen ions ($n_{O^+} = 20, 40, 60, 80$) cm^{-3} for kappa distribution function k=2.

Conclusion

In this paper we have seen the Effect of different plasma densities with different values of kappa distribution function on electrostatic ion cyclotron waves in Multi- Ions Plasma and also see the perpendicular and parallel resonant energy correspondingly. For minimum value of kappa distribution (k=1) and decreasing the value of plasma densities of different ions we get maximum growth rate with respect to particular value of wave vector after that it goes zero for all plasma densities of different ions (hydrogen, helium and oxygen ions). For maximum value of kappa distribution (k=2) and increasing the value of plasma densities of different ions we get minimum growth rate with respect to wave vector after that it goes zero for all plasma densities of different ions. This implies that we get growth rate on negative direction for all value of plasma densities of different ions.

We found that for all value of kappa, parallel resonant energy increases according to wave vector with increasing of plasma densities of ions whereas for k=1, perpendicular resonant energy increase of plasma densities of hydrogen helium and oxygen ions but for k=2 , perpendicular resonant energy is decreasing (on negative axis) with different plasma densities.

The study may be valuable for experimental devices with current carrying plasma. The particle aspect analysis established may be appropriate to laboratory plasma, as well as evaluation the heating rates along with the schoolwork of emissions of ESIC waves.

The theory may be beneficial to clarify various phenomena associated to space plasma as well as laboratory plasma. The behavior studied for the ESIC wave may be of reputation in the electrostatic emission in the auroral acceleration region. The perpendicular, parallel resonant energies and growth rate explain the wave scenario in auroral acceleration region. It is relevant to describe ESIC wave phenomena in earth's ionosphere. It was resolved from observations by fast satellite that minor ions play a dramatic role in the amendment of ESIC wave spectrum and that they can be strongly energized by the ion cyclotron waves. It is judicious to adopt that if ion cyclotron waves are existing in the solar corona, then the heavy ions will intensely affect the ion cyclotron wave spectrum.

References

1. Drummond W.E. and Rosenbluth M.N. (1962) Anomalous diffusion arising from micro-instabilities in a Plasma‖ J Phys. Fluids, 5: 1507.

2. Ahirwar,G, P Varma, and M S Tiwari (2010) Study of electromagnetic ion-cyclotron waves with general loss-cone distribution and multi-ions plasma-particle aspect approach. Ind. J. of Pure& Appl. Phys. 48: 334.
3. Temerien M, J McFadden, M Boehm, CW Carlson, and W Lotko (1986) Production of flickering aurora and field-aligned electron fluxes by electromagnetic ion cyclotron waves. J. Geophys. Res. 91: 5769.
4. Ahirwar G, P Varma, and M S Tiwari (2007) Beam effect on electromagnetic ion-cyclotron waves with general loss-cone distribution function in an anisotropic plasma-particle aspect analysis. Ann. Geophys. 25: 557.
5. Gary SP (1991) Electromagnetic ion instabilities and their consequences in space plasma. Space Sci. Rev. 56: 373.
6. Daughton W, SP Gray, and D Winske (1999) Electromagnetic proton/proton instabilities in the solar wind: Simulations. J. Geophys. Res. 104: 4657.
7. Gomberoff, L and P Vega (1990) Electrostatic instabilities driven by ion beams. Plasma Phys. Control Fusion, 32: 737.
8. Gomberoff, L and R Elgueta (1991) Resonant acceleration of alpha particles by ion cyclotron waves in the solar wind. J. Geophys. Res. 96: 9801.
9. Gnavi G, L Gomberoff, FT Gratton, and RMO Galvao (1996b) Electromagnetic ion-beam instabilities in cold plasma. J. Plasma Phys., 55: 77.
10. Gomberoff, L and HF Astudillo (1998) Electromagnetic ion-beam plasma instabilities. Planet, Space Sci., 46: 1683.
11. Mishra KD and MS Tiwari (1979) Particle aspect analysis of electromagnetic ion cyclotron instability. Con. J. Phys. 57: 1124.
12. Hamrin M, Norquist P, Hellstorm T, Andre M & Eriksson AI (2002) A statistical study of ion energization at 1700 km in the auroral region‖ Ann Geophys., 20: 1998.
13. Albert JM (2003) Evaluation of quasi-linear diffusion coefficients for EMIC waves in multispecies Plasma‖ J Geophys Res, 108(A6): 1249, Doi: 10.1029/2002JA009792.